SCIENCE CHINA
Chemistry

• REVIEWS •

December 2011 Vol.54 No.12: 1867–1876
doi: 10.1007/s11426-011-4441-5

# Early stages of non-classic crystal growth

GREER Heather F., YU FengJiao & ZHOU WuZong*

*EaStChem, School of Chemistry, University of St Andrews, Fife, KY16 9ST, United Kingdom*

Received August 9, 2011; accepted September 13, 2011; published online November 16, 2011

Investigation of early stages of crystal growth revealed that crystal growth in some systems may not follow the classic route. In the early stages of inorganic crystal growth, precursor molecules and/or nanocrystallites may aggregate into large and disordered particles with the assistance of some polymers or biomolecules. Surface crystallization of these aggregates would then take place to form shells with high crystallinity and density, followed by an extension of the crystallization from surface to core. This so-called reversed crystal growth mechanism has been found in crystallization of several inorganic compounds including zeolites, perovskites, metals and metal oxides, and will be identified in more material systems. The establishment of this new crystal growth route gave us more freedom to control the morphology of crystals and to understand the formation mechanism of many natural minerals. This article gives a brief review of the recent research in this field by featuring some typical examples of the reversed crystal growth.

**reversed crystal growth, hollow crystals, core-shell particles, electron microscopy**

## 1 Introduction

The classical crystal growth theory was established over 100 years ago. It is well known that a crystal is developed via nucleation and the repeated attachment of atoms, molecules or ions to a single nucleus. The crystal growth rates along each crystallographic orientation are different and are proportional to the surface attachment energy, which is defined as the fraction of the total lattice energy released when a growth slice of thickness $d_{hkl}$ is attached to a growing crystal surface [1]. A large interplane d-spacing, $d_{hkl}$, normally results in a low surface energy of the corresponding {hkl} planes, leading to a slow growth rate.

The Bravais-Friedel-Donnay-Harker (BFDH) law [2–4] and the Hartman-Perdok theory [5] indicate that crystals with a polyhedral morphology are generated by slow growing faces because the fast growing faces grow out so are not displayed in the final morphology. For example, the largest d-spacing of zeolite A is $d_{200}$. Therefore, the slowest crystal growth directions are along <100> and the most stable morphology of zeolite A crystals is cubic with 6 {100} facets. It can be logically expected from the classic crystal growth route (steps 1 to 3 in Figure 1) that particles at any stage of crystal growth are single crystals. This is not always the case when we look at intermediate specimens of a crystal growth system. Furthermore, the BFDH model can not explain the formation of some novel hierarchical structures, e.g. hollow crystals.

On the other hand, the formation mechanism of crystal habits can be elucidated in another way. Curie and Wulff believed that the equilibrium shape of a free crystal is the shape that minimizes its surface free energy [6, 7]. In other words, crystal morphology does not have to have a direct relation with the crystal growth rates. For example, with little influence from the growth rates, hollow crystals can also have characteristic shapes to achieve a minimum surface energy. Curie and Wulff's mechanism is more general than the BFDH theory and gives us a better insight to understand the formation of a given crystal morphology.

Based on investigations of the early stage crystal growth of several systems, Zhou elucidated a non-classic crystal

*Corresponding author (email: wzhou@st-andrews.ac.uk)

growth route (Figure 1) [8]. In the early stages of crystal growth it is highly competitive between aggregation and the repeated attachment of building units, e.g. atoms, ions or molecules. Aggregation can take place when the particles (either nanocrystallites or precursor molecules) are small and the crystal growth is relatively slow (step 4 or 5). Since the aggregates are initially disordered, they most likely form spherical particles in a synthetic solution (step 4 or 6). This stage is followed by surface crystallization, because the surface areas, benefited from contact with the solution, thus are more active than the inner regions of the aggregates (steps 7 and 8). When the crystallization extends to the whole surface of an aggregate, the particle shows a core-shell construction comprising of a thin crystalline shell and a disordered core. A surprising feature is that a characteristic polyhedron can form at this stage, no matter how thin the shell is (step 9). Finally, the crystallization would extend from the surface to the core, via an Ostwald ripening process, to achieve a single crystal (step 10). This is the so-called reversed crystal growth route. Assuming the single-crystal shell completely covers the surface of particles, mass transportation across the shell becomes very difficult. When the low density disordered core transforms into high density crystal, a hole likely forms in each particle. Therefore, many hollow crystals may be the consequence of the reversed crystal growth route.

Herein, we review some obvious examples of crystals developed from disordered aggregates and discuss their formation mechanisms.

## 2 Non-classical crystal growth routes

The reversed crystal growth route was first introduced by a joint team at Fudan and St Andrews Universities in 2007 [9], although relevant experimental evidence was observed much earlier. Despite the short history of the reversed crystal growth mechanism numerous examples exist. This mechanism has become increasingly common in materials where structure directing agents have been incorporated into the synthesis. These make the system inhomogeneous therefore encouraging aggregation to occur in the early growth stages. Some systems put under the spotlight herein include metal nanoparticles, zeolite analcime, zeolite A, perovskite, ZnO and other hollow crystals. To determine their crystal growth mechanisms, specimens were collected over a relatively large time interval and the step-by-step investigation of their size, morphology and crystal structure of the intermediate specimens was performed mainly using powder X-ray diffraction (PXRD), scanning electron microscopy (SEM) and transmission electron microscopy (TEM).

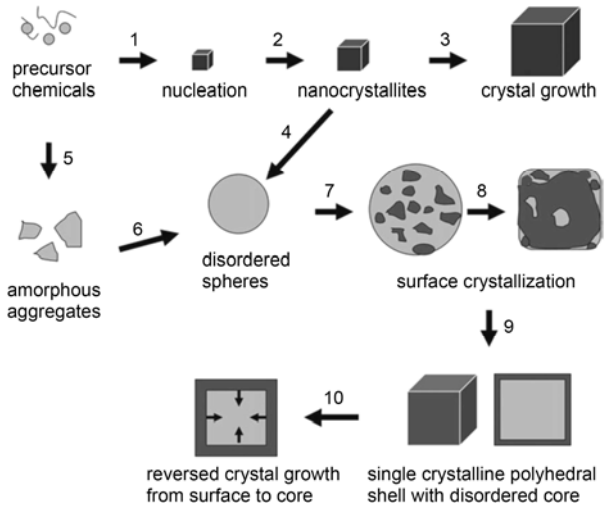


**Figure 1** Schematic illustration of the classical (steps 1–3) and the reversed crystal growth routes (steps 4–10) [8].

### 2.1 Non-classic growth of Co nanocrystallites

Metal and metallic alloy nanoparticles are important materials in many applications. We often care about the final morphology and size of these particles, but do not pay much attention to the way in which they grow up. Metallic particles normally have characteristic shapes to reflect their common cubic close packed (ccp) and hexagonal close packed (hcp) structures [10, 11]. To find the real process of metallic crystal growth, structural examination of intermediate specimens is required. This is difficult because the growth of most metal nanocrystallites is very fast and collection of the intermediate specimens is not easy.

Co-catalyzed $Mg_2SiO_4$ fishbone-like fractal nanoparticles produced by Kroto's group are special because from a single fishbone-like particle we find differently sized Co nanocrystallites on the tips of the $Mg_2SiO_4$ nanorods (Figure 2(a),(b)) [12, 13]. Therefore, we were able to examine the microstructures of Co nanoparticles with a continuous change in particle size. The results were quite amazing. Within a solid-gas reaction, Co atoms were deposited on the $Mg_2SiO_4$ surface and grew into 2 nm sized crystallites. These nanocrystallites aggregated into polycrystalline clusters instead of growing up individually (Figure 2(c)). The clusters attracted more nanocrystallites to increase their size (Figure 2(d, e)) until over 100 nm in diameter, when the clusters started to re-crystallize into single crystals (Figure 2f–h). Unfortunately, since the Co particles are very small, we could not see whether the final re-crystallization process began on the surface or the centre of clusters. In any case, the final regular polyhedral shape of the Co nanocrystallites was not directly governed by the different crystal growth rates along different orientations. Instead, it was a result of re-crystallization of each particle from polycrystalline to a single crystal state. In very recent work, we have obtained evidence of surface to core extension of crystallization in Cu/Pt alloy nanoparticles (F. J. Yu, unpublished work).

It can be seen that the early stage crystal growth is gov-

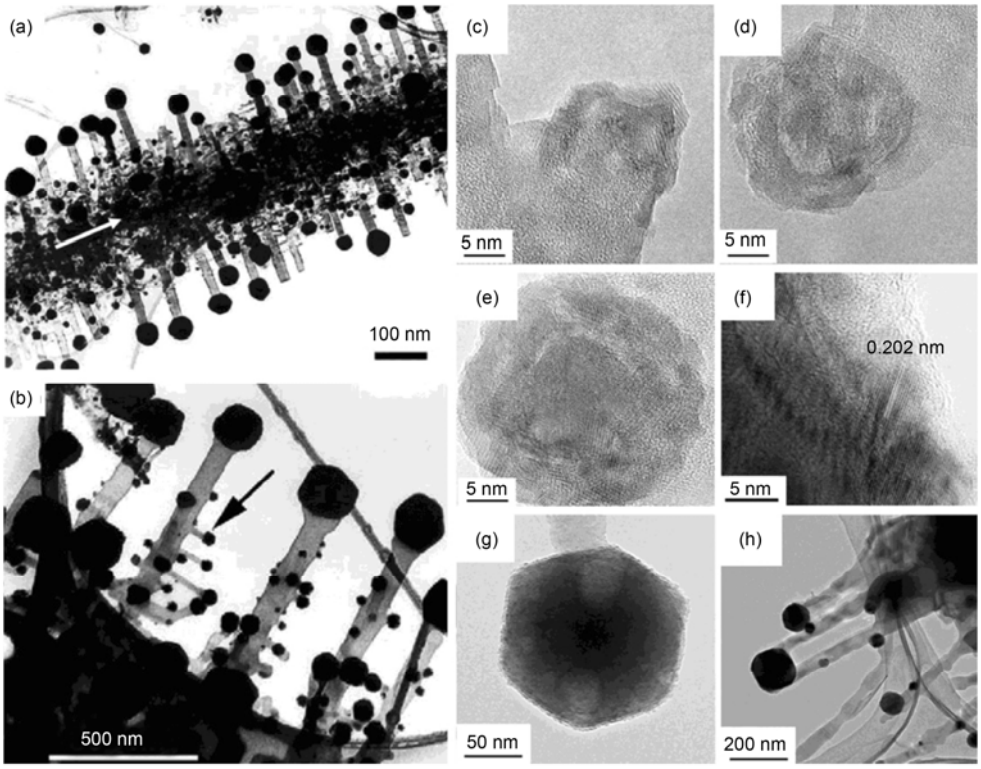


**Figure 2** (a) Low-magnification TEM image of a fishbone-like nanoparticle structure showing the main stem indicated by the arrow and secondary branches with Co catalytic nanoparticles at the top ends; (b) higher magnification TEM image showing lollipop-like secondary branches and mini-lollipop-like subsecondary branches indicated by an arrow; (c)–(e) HRTEM images of Co particles on the $Mg_2SiO_4$ surface at different growth stages; (f) HRTEM image of the edge of a polygonal Co particle, showing a large domain of single crystalline Co; (g) TEM image of a polygonal particle of Co; (h) a polygonal Co particle resulting from re-crystallization of two clusters originally located at the ends of two $Mg_2SiO_4$ branches [13].

erned by the competition between aggregation and continuous growth of individual crystallites. In the above example of Co, after forming 2 nm sized nanocrystallites, aggregation became the dominant process and the growth of individual crystallites was suppressed. The driving force of the aggregation of nanocrystallites on a solid surface has not been well understood. On the other hand, such aggregation can be found in many inorganic synthesis systems in solutions, especially those with polymers as surface protection agents where the inter-particle interaction is enhanced. One of the best examples is the growth of zeolite analcime in the presence of ethylamine [9], which is discussed below.

## 2.2 Zeolite analcime

The hydrothermal synthesis method producing zeolite analcime crystals with an icositetrahedral morphology was established at least 30 years ago [14]. It assumed the as prepared crystals followed the classic crystal growth route where nucleation is followed by the addition of atoms/ions/molecules to a single nucleus. A collaboration between scientists in Fudan and St Andrews universities namely, Chen *et al.* [9] were first to demonstrate if structure directing agents (i.e. ethylamine in the case of zeolite analcime) were incorporated into the synthesis then aggregation would occur causing the growth to go against the classic crystal growth theory. From this, a reversed route was developed where nanocrystallites aggregated into spherical particles, then surface re-crystallization created a thin crystalline shell. Surface re-crystallization extended inwards to the core resulting in an increased thickness of the crystalline layer via an Ostwald ripening process consuming the core crystallites.

The nominal molar composition in the synthesis of analcime comprised of 1 $SiO_2$ / 1 $Na_2O$ / 0.22 Ni / 0.48 Al / 1.26 $C_2H_5NH_2$ / 0.63 $H_2SO_4$ / 19 $H_2O$. The mixture was placed in a teflon-lined stainless steel autoclave at 180 °C. The reaction was stopped with specimens collected at various times between 6 h and 22 days, the microstructures were analyzed using PXRD, SEM, TEM and selected area electron diffraction (SAED).

After a reaction time of 16 h the first crystalline phase seen as analcime polygonal shaped nanoplatelets with a diameter of around 20 nm formed (Figure 3(a)). No further growth occurred on these nanoplatelets which were likely caused by the adsorption of ethylamine molecules on the principal surface (111) planes of the analcime structure. These nanocrystallites underwent orientated aggregation to form discus-shaped clusters (Figure 3(b)) with a diameter of

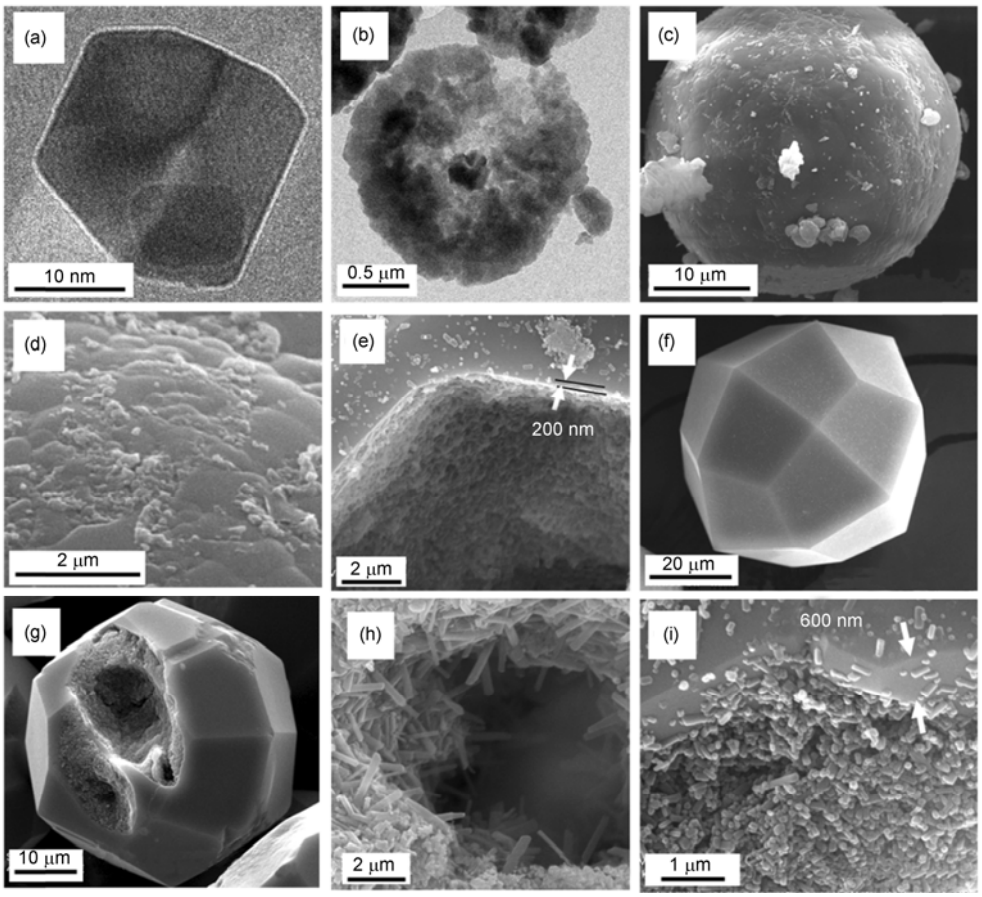


**Figure 3** Microscopic images of zeolite analcime at various stages of growth. (a) TEM image of a nanoplatelet in the 16 h sample, viewed down the [111] zone axis; (b) TEM image of a discus-shaped cluster developed from the orientated aggregation of nanoplatelets; (c) SEM image of a polycrystalline microsphere from the 20 h sample; (d) enlarged SEM image of the surface of the microsphere in (c) showing partial surface re-crystallization; (e) SEM image of a specimen from the 3 day sample displaying a 200 nm thick single crystalline shell and a polycrystalline core; (f) SEM image of a perfect icositetrahedral particle formed after hydrothermal treatment for 8 days; (g) SEM image of an intentionally broken icositetrahedron, showing nanorods (h) in the core; (i) polyhedral crystal with a 600 nm thick shell generated after hydrothermal treatment for 8 days [9].

approximately 1–2 μm. Single-crystal like SAED patterns could be observed from these clusters [9], although the particles did not look like single crystals at all with obvious boundaries between nanoplatelets as shown in the TEM image of Figure 3(b).

The perfectly orientated aggregation of the nanoplatelets could only occur when the manner of stacking of the nanoplatelets was highly selective. In other words, when two nanoplatelets stack face to face along the [111] direction, they would self-adjust their orientations to achieve the maximum number of chemical bonds. All other non-orientated interactions will not result in stable stacking. To prove this assumption, computer simulation of the inter-particle interactions is necessary.

At a reaction time of 20 h the discus-shaped clusters had further aggregated into larger polycrystalline microspheres of about 20–30 μm in diameter (Figure 3(c)). When closely inspecting the surface of the microspheres using SEM imaging they were found to be notably rough and contained no icositetrahedral facets. Evidence of surface re-crystallization was observed by the many nano-sized pieces of crystalline "islands" on the surface (Figure 3(d)). The large smooth domains led to the assumption that when the reaction time was extended the coverage of crystalline "islands" increased. These nano-sized pieces of crystalline material fused together to encase the entire microsphere after their orientation had been adjusted to form the 24 identical {211} facets of an icositetrahedron. There is no reason to say the separated crystalline "islands" have coordinated orientations. They are also unlikely to be mobile on the surface of the microspheres. How they self-adjust their orientations to form 24 identical {211} facets of an icositetrahedron still remains mysterious.

The icositetrahedral morphology was first detected in the 3 day specimen although the facets were still considerably rough. Surface re-crystallization had converted the surface of the microspheres into a very thin single crystalline shell (Figure 3(e)). The crystals with a hydrothermal treatment time of 8 days were perfectly smooth icositetrahedral shaped crystals as demonstrated in Figure 3(f). However, it

was very surprising that perfect icositetrahedral crystals do not always mean that the crystal is a single crystal. When the perfect icositetrahedral particles were crushed (Figure 3(g)), SEM images revealed a polycrystalline core filled with a large number of randomly orientated analcime nanorods (Figure 3(h)). The thickness of the single crystalline shells increased on extending the growth time (Figure 3(i)) by consuming the nanorods in the cores through an Ostwald ripening process until hollow single crystalline icositetrahedral microparticles were produced. The above crystal growth process was named the NARS route for short, after a process of Nanocrystallites, orientated Aggregation, surface Re-crystallization and Single crystal via surface-to-core reversed crystal growth. Soon after this discovery, zeolite A was chosen to confirm if it followed a similar mechanism or if in fact the NARS route was a one-off discovery.

### 2.3 Zeolite A

Zeolite A (LTA) is one of the most widely manufactured zeolites for its applications in ion-exchange, adsorption and medical applications [15–17]. For many years cubic single crystalline zeolite A particles were synthesized using the classic crystal growth method [18]. Yao *et al*. changed the growth route by adding biopolymer chitosan as a non-structure directing agent [19]. Chitosan polymers are natural amino polysaccharides derived from the exoskeleton of crustaceans such as shrimp and crabs [20]. Cubic zeolite A crystals were synthesized by adding an alkaline solution of $Na_2O/Al_2O_3/H_2O$ to silica dispersed in an acidified chitosan solution resulting in sodium aluminosilicate entrapped in a uncrosslinked chitosan hydrogel. The gel was sealed, aged for 18 h then hydothermally treated at 90 °C for 3 h. Initially, Yao *et al*. expected many uniform nano-sized zeolite crystals. Instead many cubic crystals with a diameter of 1–2

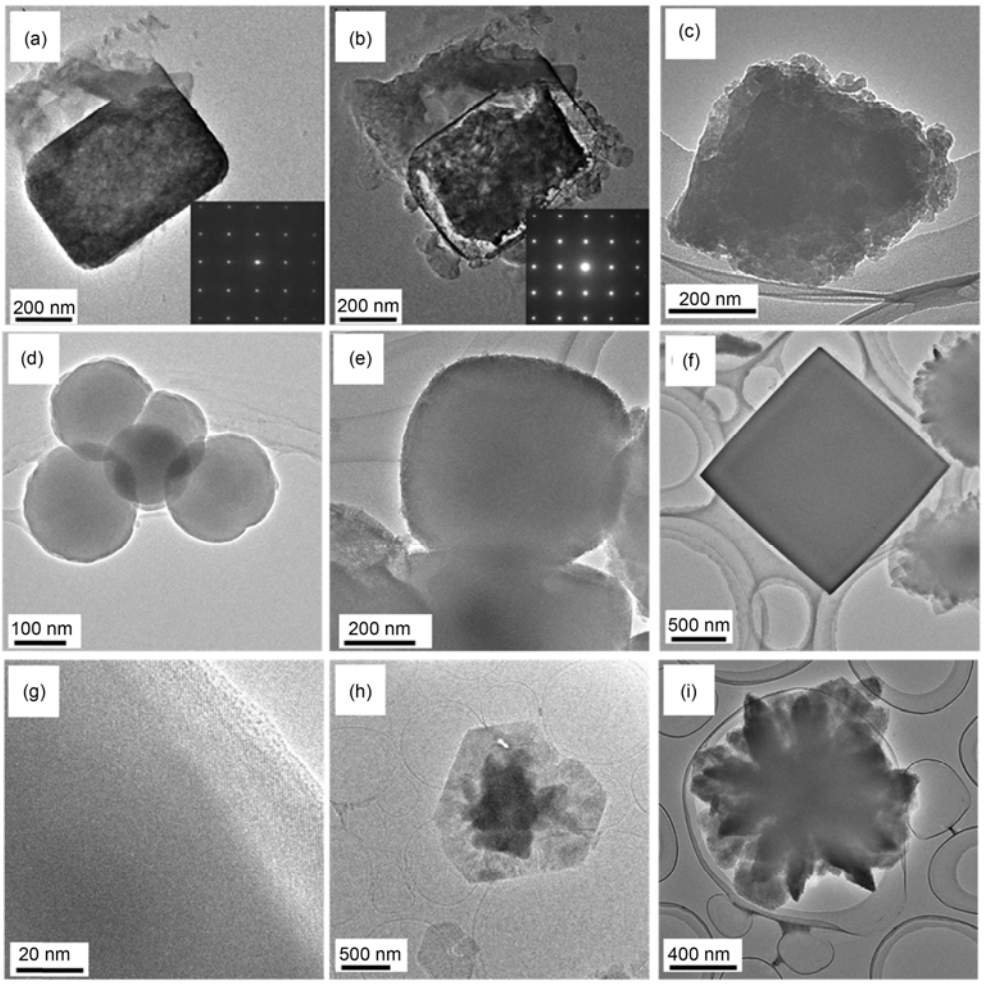


**Figure 4** TEM images of the early stage crystal growth of core-shell zeolite A crystals and their phase transformation to zeolite sodalite. (a) Zeolite A crystal after crystal growth of 3 h; (b) the same particle after annealing with the electron beam for a few minutes. Insets are the corresponding SAED patterns; (c) irregular shaped aggregates from the 0.5 h specimen; (d) amorphous spherical particles developed after crystal growth of 1 h; (e) TEM of a 1 h crystal with a morphology between spherical and cubic; (f) perfect cubic zeolite A crystal from the 3 h sample; (g) HRTEM image of the edge of a cubic zeolite A particle showing a crystalline shell and an amorphous core; (h) crystal from the 168 h specimen showing evidence of sodalite plates forming in the centre of a cubic crystal; (i) pure sodalite crystal from the 168 h sample [19, 21].

μm were produced which, according to the PXRD pattern, exhibited a weak crystallinity, implying a large proportion of the particles were amorphous.

The core-shell structure was proved by TEM imaging before and after annealing (Figure 4(a), (b)) a zeolite A crystal with a weak electron beam for a few minutes. After beam irradiation the core became more disordered than before, reduced in volume and separated itself from the shell. Single crystalline SAED patterns taken down the [001] viewing direction of the LTA crystal structure before and after annealing were almost identical, indicating the crystalline structure of the shell remained intact. No extra diffraction spots were observed signifying the crystals have an amorphous core rather than polycrystalline. The joint team at Monash University and University of St Andrews reported that the core material could be removed by acidic treatment to produce hollow cubes of zeolite A [19].

To confirm if these core-shell cubic crystals developed by aggregation and surface crystallization, the step-by-step analysis of specimens with a hydrothermal treatment time lower than 3 h was performed by Greer *et al*. [21]. Precursor and chitosan molecules aggregated into irregular and spherical particles (Figure 4(c), (d)). The spherical morphology was then gradually changed to a cubic shape with a diameter of 1–2 μm (Figure 4(e), (f)). It is thought that the morphology change to cubic crystals with six {100} facets occurred by a similar process to analcime as discussed above. This process converted the surface of the cubes into a thin single crystalline shell whilst the core remained amorphous. Further evidence of the core-shell structure was found when HRTEM was performed on the edge of a perfect cube in the 3 h specimen (Figure 4(g)). HRTEM imaging at a magnification of 200,000 times gave clear evidence of surface crystallisation when a 24 nm thick crystalline surface coating layer was observed. Like in zeolite analcime it was expected that upon increasing the hydrothermal treatment time hollow cubic zeolite crystals with a relatively thick shell would be prepared. However, this never occurred in zeolite A; instead, the surface to core re-crystallisation resulted in an increase of pressure in the core of the cubes leading to nucleation of zeolite sodalite. At approximately 72 h these sodalite plates developed in the amorphous cores which eventually broke the cubic shells when the reaction time was increased (Figure 4(h)). Eventually a complete phase transformation to sodalite occurred (Figure 4(i)).

The more general applicability of the reversed crystal growth route is further validated by its presence in metal oxides. Some typical examples are discussed below.

### 2.4 Perovskite $CaTiO_3$

Calcium titanate is an important mineral in many fields such as solid-state chemistry [22], biotechnology [23], and other applications in sensor devices and in solid oxide fuel cells [24]. Wu and co-workers at Sun Yat-Sen (Zhongshan) University synthesized $CaTiO_3$ crystals using a water-free poly(ethylene glycol) (PEG-200) solution [25]. Hollow crystals exhibiting a walnut-like morphology and an average size of 600 nm formed after hydrothermal treatment for 15 h. Adding small amount of water in the synthetic system led to hollow cubic crystals.

Stopping the reaction in the very early growth stages found calcium titanite nanocubes with a diameter of a few nanometres formed first. Further growth of the individual nanocubes did not take place. Instead, these nanocubes underwent an orientated aggregation process to form spherical polycrystalline particles (Figure 5(a)). It is thought when the PEG-200 polymer molecules absorbed on the $\{100\}_c$ surfaces of the nanocubes, this enhanced their ability to undergo the orientated assembly. TEM images (Figure 5(a–c)) of aggregates prepared with extended hydrothermal treatment times found their size increased from 90 nm at 1 h to 150 nm at 3 h and then finally to 600 nm at 5 h. SAED patterns taken from specimens are single-crystal like, although the particles were still aggregates of nanocubes.

Nanocubes near the outer surface of the 5 h specimens were discovered to be significantly larger than those in the core. This implies that the nanocubes near the surface of the particles grew further by consuming the small cubes in the cores via Ostwald ripening. The density of the surface area gradually increased, while the density of the core decreased. Consequently, a hole appeared in the centre of each particle (Figure 5(c, d)). By increasing the water content to 5% in the synthetic solution, single crystalline cubic shells of $CaTiO_3$ were produced.

This research performed by an international collaboration

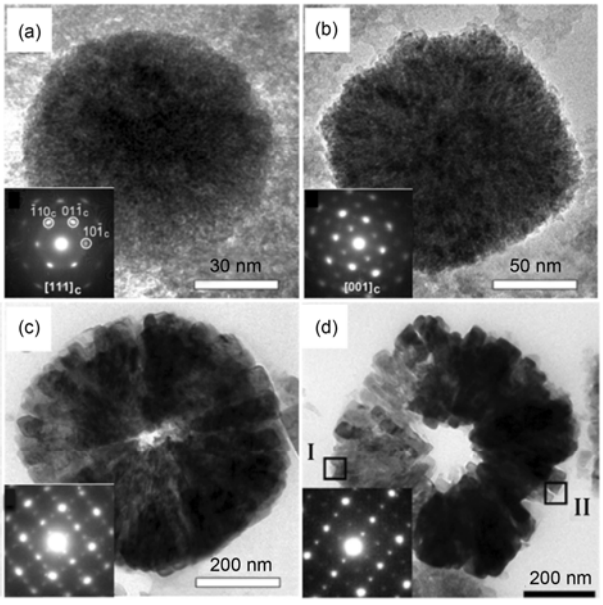


**Figure 5** TEM images of $CaTiO_3$ particles after a crystal growth time of (a) 1 h, (b) 3 h, (c) 5 h, and (d) 15 h. Inset are the corresponding SAED patterns [25]. I and II are the areas examined by HRTEM imaging to reveal the nanocubic building units and perfectly orientated aggregation [25].

between two groups in Sun Yat-Sen and St Andrews Universities revealed yet again a general process of the formation of hollow crystals.

### 2.5 ZnO twin-crystals

Recently, the biomimetic synthesis of inorganic crystals has attracted a lot of attention for its fine control over morphologies [26, 27]. This combined with the sought-after properties attributing to wurtzite ZnO make research on the biomimetic ZnO twin crystals very important. All biomimetic syntheses require addition of a surfactant or polymer to act as a structure directing agent so nucleation and the build-up of crystallites can be stringently controlled. Mou and co-workers prepared hierarchical ZnO twin crystals by hydrothermal treatment, where gelatin (type B) was incorporated as the structure directing agent (Figure 6) [28]. Gelatin type B is a single chain series of repeating amino acids obtained from the thermal denaturation of collagen under alkaline conditions [29]. The well-defined twin-crystal morphology was found to be built from the stacking of nanoplates (150–400 nm in diameter and 20-50 nm in thickness) in a parallel manner along the c-direction (Top inset of Figure 6). To understand the formation mechanism of these twin crystals, the microstructure of the central cores of the particles must be investigated. The origin of the twin crystals can only be revealed by a step-by-step investigation of the crystal growth starting at the very early growth stages.

More recently, Greer *et al.* [30] prepared ZnO specimens using identical conditions but varying the hydrothermal treatment time from 10 min to 21 h. It was found that nanoplatelet shaped monoclinic $Zn_5(NO_3)_2(OH)_8{\cdot}2H_2O$ was the first crystalline phase to appear in the synthetic system. These nanoplatelets underwent orientated aggregation with gelatin molecules to form mesocrystalline $Zn_5(NO_3)_2$-$(OH)_8{\cdot}2H_2O$/gelatin nanoplates. The inclusion of gelatin molecules in the nanoplates is accountable for their porous nature. HRTEM imaging of the well-orientated nanoplates found a pseudo-hexagonal intra-domain atomic structure on the (100) projection in $Zn_5(NO_3)_2(OH)_8{\cdot}2H_2O$. Surface re-crystallization into ZnO took place on some nanoplates with the crystallization extending from both surfaces towards the centre, forming double-layer nanoplates. Re-crystallization continued inwards, increasing the thickness of the ZnO layers until all $Zn_5(NO_3)_2(OH)_8{\cdot}2H_2O$ particles were consumed. By looking at the profile projection some single layer nanoparticles now appear as double-layer nanoplates.

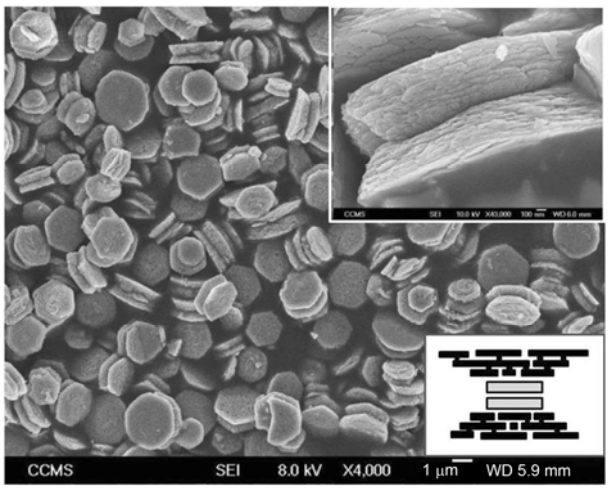


**Figure 6** SEM image of ZnO twin-crystals. Top inset: large magnification SEM image of a twin-crystal. Bottom inset: a model of the core structure of the twin-crystals.

These double-layer nanoplates served as the cores (or the origin) of the ZnO twin crystals, which were constructed by deposition of single-layer nanoplates on both sides of the cores (bottom inset of Figure 6). It is interesting to find that the process of aggregation, surface re-crystallization and reversed growth extension was observed again in the formation of core particles of ZnO twin-crystals at a nanometer scale.

As presented above, the reversed crystal growth route often leads to core-shell structures and, eventually, hollow crystals, which have widespread interest due to their potential applications as chemical reactors, drug-delivery carriers and heterogeneous catalysts [31–33]. However, the formation mechanisms of these particles were not fully understood for many years. The newly established reversed crystal growth route allows us to elucidate the growth mechanisms of these hollow crystals much more appropriately.

### 2.6 Some more recent examples of hollow crystals

Wu and co-workers demonstrated a "templating and surface to core" crystallization mechanism with hollow zeolite ZSM-5 (MFI) microspheres, which were synthesized through an in situ transformation of mesoporous silica spheres into this MFI-type zeolite in the presence of isopropylamine as a structure-directing agent (Figure 7) [34]. The original spheres were disordered mesoporous silica (Figure 7(a), (b)). The surface of the microsphere then crystallized into a high density shell consisting of MFI nanocrystallites (Figure 7(c), (d)). The silica and alumina species in the core condensed and crystallized to ZSM-5 thereafter, forming microcrystals inside the spheres. These microcrystals aggregated on the inner surface of the shell to form hollow spheres (Figures 7(e), (f)). In this synthetic system, surface crystallization did not lead to the single-crystalline shell. This was why the spherical morphology was maintained instead of forming polyhedral shells. Nevertheless, the authors mentioned the reversed crystal growth mechanism and believed that "The present work may provide indirect evidence for such crystal growth route, and would be surely beneficial to the design and fabrication of zeolite spheres."

In order to elucidate the formation mechanism of hollow NaP zeolite particles synthesized using a vapor-phase-

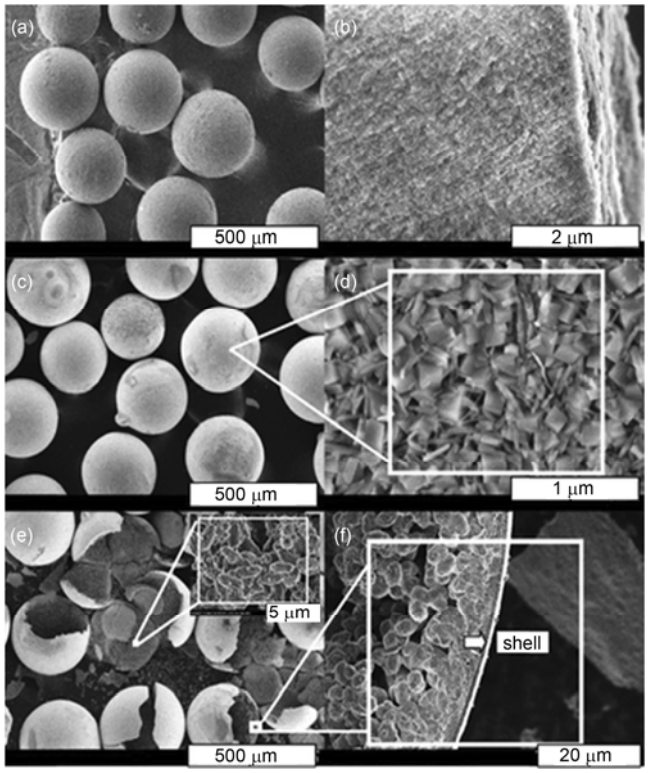


**Figure 7** SEM images of specimens showing the formation of ZSM-5 hollow spheres, (a) overview and (b) inside the spheres of parent mesoporous silica spheres, (c) overview, (d) enlarged image of the surface of ZSM-5 spheres, (e) hollow structure after crushing, (f) a profile view of the sphere shell [34]. Reproduced by permission of The Royal Society of Chemistry.

transport (VPT) method, Wang and co-workers also believed the reversed crystal growth route was responsible for the formation of the hole [35]. At an early stage, pseudo-spherical particles formed by self-assembly of zeolite gel particles. They then explained that the initial nucleation occurred on the surface of the particles to form crystalline shells because the gel particles on the sphere surface had preferential and sufficient contact with water vapour in the VPT environment. Hollow structures were achieved by consuming the gel particles in the cores via a solution-mediated process.

More perovskite-type materials were found to be in hollow in structure. For example, perovskite $SrZrO_3$ with hollow cuboidal nanoshells were synthesized recently via a simple hydrothermal route from concentrated KOH solutions without any organic or inorganic templates [36]. The particle size could be tuned by simply adjusting the base concentration, implying the base reduced the interaction between the precursor molecules/ions, leading to smaller particle sizes. It was believed that the nanoshells were formed via the reversed crystal growth as observed from $CaTiO_3$ [25], although the very small nanocubic building units were not identified and the driving force for aggregation at early stage was not fully understood.

If reversed crystal growth takes place in plate-shaped particles (2D), as we discussed above for the ZnO twin-crystals, double-layer plates with a low density central layer would be the resultant morphology. When this happens in 1D materials a tubular morphology would be produced. Choi and co-workers attributed the formation of CuS nanotubes from $[Cu(tu)]Cl{\cdot}1/2H_2O$ nanowires to the reversed crystal growth route [37].

## 3 Conclusion

The discovery of the reversed crystal growth route widens current knowledge on crystal growth and provides a new avenue to understand and re-consider the formation of many crystalline materials. In some synthesis systems, precursor chemicals or nanocrystallites intend to join together to form disordered large particles before the individual crystals grow up. Classic crystal growth will therefore be disturbed. Instead, surface crystallization on these aggregates may occur, followed by surface-to-core reversed crystal growth. This non-classic growth route often brings in many complicated intermediate mesostructures in between nucleation and final single-crystalline products. Two most common and interesting mesostructures are core-shell particles and hollow crystals, both have wide potential applications in industry. In addition, the aggregation and re-crystallization process is often found in biomimetic syntheses. Understanding the details of crystal growth is crucial in order to study the geometries of the materials.

There are many fundamental scientific problems left in this field, e.g. interaction between the chemicals in initial aggregates, driving force of orientated assembly, calculation of surface energy of crystals in a solution, etc. Materials characterisation is not sufficient for solving all these problems. Computational chemists would probably be of great help.

*The authors would like to thank EaStCHEM and University of St Andrews for a studentship to H.F.G., to Sasol for financial support and University of St Andrews for an ORS award to F.J.Y. The authors are also grateful to The Royal Society for an International Collaboration Grant, and to Professors Heyong He of Fudan University, Huanting Wang of Monash University, M.M. Wu of Zhongshan University and C.-Y. Mou of National Taiwan University for their fruitful collaborations in this field.*

1 Docherty R, Clydesdale G, Roberts KJ, Bennema P. Application of Bravais-Friedel-Donnay-Harker, attachment energy and Ising models to predicting and understanding the morphology of molecular crystals. *J Phys D: Appl Phys*,1991, 24: 89–99
2 Bravais A. *Études Crystallographic*. Paris: Gauthier-Villars, 1866
3 Friedel MG. Étudessurla loi de Bravais. *Bull Soc Fr Mineral Cristallogr*, 1907, 30: 326–455
4 Donnay D, Harker D. A new law of crystal morphology extending the law of bravais. *Am Mineral*, 1937, 22: 446–467
5 Hartman P, Perdok WG. On the relations between structure and morphology of crystals. II. *Acta Crystallogr*, 1955, 8: 521–524

6 Curie P. Sur la formation des cristaux et sur les constants capillaires de leursdifférentes faces. *Bull Soc Fr Mineral Cristallogr*, 1885, 8: 145–150
7 Wulff G. Zur frage der geschwindigkeit des wachstums und der auflösung der kristallflächen. *Z Kristallogr*, 1901, 34: 449–530
8 Zhou WZ. Reversed crystal growth: Implications for crystal engineering. *Adv Mater*, 2010, 22: 3086–3092
9 Chen X, Qiao M, Xie S, Fan K, Zhou WZ, He H. Self-construction of core-shell and hollow zeolite analcime icositetrahedra: a reversed crystal growth process via recrystallization from surface to core. *J Am Chem Soc*, 2007, 129: 13305–13312
10 Tao A, Sinsermsuksakul P, Yang PD. Polyhedral silver nanocrystals with distinct scattering signatures. *Angew Chem Int Ed*, 2006, 45: 4597–4601
11 Niu ZQ, Peng Q, Gong M, Rong HP, Li YD. Oleylamine-mediated shape evolution of palladium nanocrystals. *Angew Chem Int Ed*, 2011, 50: 1–6
12 Zhu YQ, Hsu WK, Zhou WZ, Terrones M, Kroto HW, Walton DRM. Selective co–catalysed growth of novel MgO fishbone fractal nanostructures. *Chem Phys Lett*, 2001, 347: 337–343
13 Xie SH, Zhou WZ, Zhu YQ. Formation mechanism of $Mg_2SiO_4$ fishbone-like fractal nanostructures. *J Phys Chem B*, 2004, 108: 11561–11566
14 Ueda S, Koizumi M. Crystallization of analcime solid solutions from aqueous solutions. *Amer Mineral*, 1979, 64: 172–179
15 Hui KS, Chao CYH, Kot SC. Removal of mixed heavy metal ions in wastewater by zeolite 4A and residual products from recycled coal fly ash. *J Hazard Mater*, 2005, 127: 89–101
16 Moore TT, Koros WJ. Sorption in zeolites modified for use in organic-inorganic hybrid membranes. *Ind Eng Chem Res*, 2008, 47: 591–598
17 Mowbray M, Tan X, Wheatley PS, Morris RE, Weller RB. Topically applied nitric oxide induces T-lymphocyte infiltration in human skin, but minimal inflammation. *J Invest Dermatol*, 2008, 128: 352–360
18 Robson H, Lillerud KP. Verified syntheses of zeolitic materials. Elsevier, Amsterdam, 2001
19 Yao J, Li D, Zhang X, Kong CH, Yue W, Zhou WZ, Wang H. Cubes of zeolite A with an amorphous core. *Angew Chem Int Ed*, 2008, 47: 8397–8399
20 Pillai CKS, Paul W, Sharma CP. Chitin and chitosan polymers: chemistry, solubility and fiber formation. *Prog Polym Sci*, 2009, 34: 641–687
21 Greer HF, Wheatley PS, Ashbrook SE, Morris RE, Zhou WZ. Early stage crystal growth of Zeolite A and its phase transformation to sodalite. *J Am Chem Soc*, 2009, 131: 17986–17992
22 Mather GC, Islam MS, Figueirdo FM. Atomistic study of a $CaTiO_3$-based mixed conductor: Defects, nanoscale clusters, and oxide-ion migration. *Adv Funct Mater*, 2007, 17: 905–912
23 Inoue M, Rodriguez AP, Takagi T, Katase N, Kubota M, Nagai N, Nagatsuka H, Nagaoka N, Takagi S, Suzuki K. Effect of a new titanium coating material ($CaTiO_3$-aC) prepared by thermal decomposition method on osteoblastic cell response. *J Biomater Appl,* 2010, 24: 657–672
24 Navrotsky A, Weidner DJ. Perovskite: A structure of great interest to geophysics and materials science. American Geophysical Union, 1989, Geophysical Monograph
25 Yang X, Fu J, Jin C, Chen J, Liang C, Wu M, Zhou WZ. Formation mechanism of $CaTiO_3$ hollow crystals with different microstructures. *J Am Chem Soc*, 2010, 132: 14279–14287
26 Meldrum FC, Cölfen H. Controlling mineral morphologies and structures in biological and synthetic systems. *Chem Rev*, 2008, 108: 4332–4432
27 Chen C-L, Rosi NL. Peptide-based methods for the preparation of nanostructured inorganic materials. *Angew Chem Int Ed*, 2010, 49: 1924–1942
28 Tseng YH, Lin HY, Liu MH, Chen YF, Mou CY. Biomimetic synthesis of nacrelike faceted mesocrystals of ZnO-gelatin composite. *J Phys Chem C*, 2009, 113: 18053–18061
29 Bauermann LP, Campo A del, Bill J, Aldinger F. Hetergeneous nucleation of ZnO using gelatin as the organic matrix. *Chem Mater*, 2006, 18: 2016–2020
30 Greer HF, Zhou WZ, Liu MH, Tseng YH, Mou CY. The origin of ZnO twin crystals in bio-inspired synthesis. *CrystEngComm*, 2011, in press
31 Yin Y, Rioux RM, Erdonmez CK, Hughes S, Somorjai GA, Alivisatos AP. Formation of hollow nanocrystals through the nanoscale-kirkendall effect. *Science*, 2004, 304: 711–714
32 Kawashima Y, Niwa T, Takeuchi H, Hino T, Itoh Y. Hollow microspheres for use as a floating controlled drug delivery system in the stomach. *J Pharm Sci*, 1992, 81: 135–140
33 Morris CA, Anderson ML, Stroud RM, Merzbacher CI, Rolison DR. Silica sol as a nanoglue: flexible synthesis of composite aerogels. *Science*, 1999, 284: 622–624
34 Wang Z, Liu Y, Jiang J, He M, Wu P. Synthesis of ZSM-5 zeolite hollow spheres with a core/shell structure. *J Mater Chem*, 2010, 20: 10193–10199
35 Huang Y, Dong D, Yao J, He L, Ho J, Kong C, Hills AJ, Wang H. In situ crystallization of macroporous monoliths with hollow NaP zeolite structure. *Chem Mater*, 2010, 22: 5271–5278
36 Ye T, Dong Z, Zhao Y, Yu J, Wang F, Guo S, Zou Y. Controllable fabrication of perovskite $SrZrO_3$ hollow cuboidal nanoshells. *CrystEngComm*, 2011, 13: 3842–3847
37 Mao J, Shu Q, Wen Y, Yuan H, Xiao D, Choi MMF. Facile fabrication of porous CuSnanotubes using well-aligned[Cu(tu)]Cl·1/2$H_2O$ nanowire precursors as self-sacrificial templates. *Cryst Growth Des*, 2009, 9: 2546–2548

**GREER Heather F**. received her B.Sc in Chemistry and Mathematics at the University of St Andrews in 2009. She is currently a Ph.D. student at the University of St Andrews under the supervision of Professor WuZong Zhou. Her current research interests are the early stage crystal growth and reversed crystal growth of various microporous and mesoporous materials.

**YU Feng,Jiao** received a B.Sc degree from Fudan University in 2010. She is working as a Ph. D. student in Professor Wuzong Zhou's group in University of St Andrews. Her research interest centers on growth mechanism and structure of nanomaterials.

**ZHOU WuZong** is a Professor of Chemistry at University of St Andrews. He obtained his B.Sc in chemistry in 1982 from Fudan University, Shanghai. He started his research in HRTEM characterisation of solids in 1984 in University of Cambridge under the supervision of Dr. David A. Jefferson and Professor Sir John M. Thomas, and received his Ph.D. in 1988. He then continued his research work in Cambridge, as a postdoctoral researcher in the Department of Chemistry, a Research Fellow in Queens' College (1987–1990) and Assistant Director of Research (1993–1998). In 1999, he moved to St Andrews University to set up the Electron Microscopy Laboratory. His current research interests are the synthesis and characterisation of nanomaterials and porous materials, and the investigation of early stage crystal growth.